J. Fluid Mech. (2006), *vol.* 555, *pp.* 59–80.
doi:10.1017/S0022112006008755 Printed in the United Kingdom

Laminar capillary flow of compressible viscous fluids

By DAVID C. VENERUS

Department of Chemical Engineering and Center of Excellence in Polymer Science and Engineering, Illinois Institute of Technology, Chicago, IL 60616, USA

(Received 4 March 2005 and in revised form 22 September 2005)

Laminar flow of compressible Newtonian fluids in capillaries is analysed. A perturbation solution is obtained to the vorticity–stream function form of the hydrodynamics equations for weakly compressible flow, having a relatively simple form. In contrast with previous analyses of this flow, we find both a non-zero radial velocity and non-zero radial pressure gradient. Expressions for pressure drop and friction factor are also found that show significant deviations from the incompressible case (Hagen–Poiseuille equation) that arise from both fluid inertia and bulk viscosity.

1. Introduction

Laminar flow in a circular tube is perhaps the most commonly encountered and widely studied problem in fluid mechanics. Experimental (Hagen 1839; Poiseuille 1841) and theoretical (Stokes 1845; Hagenbach 1860) studies of capillary flow have a long history dating back to the middle of the 19th century. For steady, laminar flow of an incompressible Newtonian fluid of viscosity μ and density ρ_0 in a capillary of length L and radius R, the following relation holds:

$$W = \frac{\rho_0 \pi R^4 \Delta P}{8\mu L}$$

where W is the mass flow rate and ΔP is the pressure drop over the length of the capillary. This equation, commonly referred to as the 'Hagen–Poiseuille equation,' is an invaluable tool for the design of pipeline systems or for the analysis of capillary viscometer experiments. In some cases, it is more convenient to use a friction factor f, which is a dimensionless drag force on the capillary wall. In terms of the Darcy friction factor, the Hagen–Poiseuille equation can be written as

$$f = \frac{32}{Re}$$

where $Re = W/\pi R\mu \lesssim 10^3$ is the criterion for laminar flow in a capillary. (Note that this definition for Re is one-half the conventional definition using pipe diameter $2R$.)

The Hagen–Poiseuille equation is derived assuming fully developed, isothermal flow, and that the fluid properties (i.e. density and viscosity) are constant. For many situations, such as the flow of water and organic liquids in ordinary-sized capillaries and tubes, these assumptions are justified. For the flow of gases, however, in long capillaries or at high speeds, the assumption that the fluid is incompressible is no longer valid. The majority of work addressing the effect of compressibility in flow

through capillaries has focused on gas flows where viscous effects are of secondary importance (Shapiro 1953).

Situations where viscous effects and fluid compressibility are important include flow through micro-capillaries and the flow of super-critical fluids and highly viscous liquids. For example, pressure drops of $\sim$10 MPa are encountered in capillary viscometry of polymeric liquids for capillaries with $L/R \sim 10$ (Macosko 1994). Not surprisingly, flows of polymer liquids through capillaries show significant deviations from the Hagen–Poiseuille equation. However, even if the non-Newtonian nature of the fluid is taken into account, significant differences between experiment and theory remain. It is not clear whether these discrepancies are due to viscous dissipation, compressibility, wall slip, or other factors (Macosko 1994). Flows of gases and low-viscosity liquids in micro-tubes and capillaries ($R \sim 10\,\mu$m) also show significant deviations from the Hagen–Poiseuille equation (Beskok, Karniadakis & Timmer 1996; Gad-el-Hak 1999; Ho & Tai 1998). Several factors are thought to be responsible for the deviations observed in micro-tube and micro-channel flows, including rarefaction (slip), compressibility, surface roughness and electro-kinetic forces. However, the high uncertainty inherent in experimental techniques for studying flows in micro-devices has precluded attempts to determine the relative importance of these different factors (Papautsky, Ameel & Fraizer 2001).

There are surprisingly few theoretical analyses of the flow of compressible viscous fluids in capillaries. Prud'home, Chapman & Bowen (1986) and van den Berg, ten Seldam & van der Gulik (1993*a*) found approximate analytical solutions of the hydrodynamic equations using the lubrication approximation. These solutions are expected to be sufficiently accurate for slow flow or flow in long capillaries (i.e. $R/L \ll 1$). Zohar *et al.* (2002) adopted the approach used by van den Berg *et al.* (1993*a*) to describe gas flows through micro-tubes and channels with wall slip. Guo & Wu (1997, 1998) obtained numerical solutions of a simplified, two-dimensional form of the hydrodynamic equations for compressible gas flow in a capillary. However, the limited results presented in these papers were insufficient to assess the validity of the lubrication approximation (Guo & Wu 1997, 1998).

In the present study, we analyse capillary flow of compressible Newtonian fluids without the lubrication approximation. With this analysis, the effect of compressibility on two-dimensional velocity and pressure fields is investigated. Expressions for pressure drop and friction factor for the flow of compressible Newtonian fluids in capillaries are presented. The present analysis also allows us to examine the validity of approximations commonly employed to analyse this flow. The hydrodynamic equations governing capillary flow of compressible viscous fluids, including the vorticity–stream function formulation, are developed in § 2. The perturbation approach used to find an analytical solution valid in the weakly compressible limit is described in § 3. In § 4, we present solutions obtained using different approximations methods. The results of the analysis are presented and discussed in § 5; conclusions of the study are given in § 6.

2. Hydrodynamic equations

We consider the steady laminar flow of a compressible Newtonian fluid with constant viscosity μ and bulk viscosity ζ in a capillary of radius R and length L (see figure 1). For this analysis, we assume the flow is isothermal; criteria for the validity of this assumption are given in the Appendix. The fluid density is assumed to be a linear

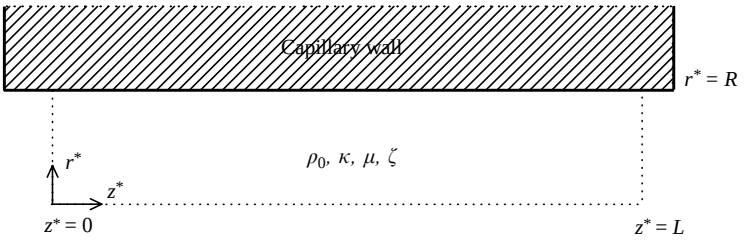

FIGURE 1. Schematic of compressible capillary flow geometry. $r = r^*/R$; $\bar{z} = z^*/L$.

function of pressure with compressibility κ. We assume there is no circumferential flow, there is symmetry about the axial coordinate and that gravitational effects are negligible. The capillary wall is impermeable and we assume there is no slip at the fluid/capillary-wall interface.

The governing equations are made dimensionless using characteristic quantities associated with the flow of an incompressible fluid of density ρ_0 and viscosity μ with mass flow rate W. Hence, spatial positions are scaled by R, density by ρ_0 and velocities by $W/\rho_0\pi R^2$. Pressure, relative to P_0, a reference pressure at the capillary wall exit, is scaled by $8\mu LW/\rho_0\pi R^4$. The assumptions stated above lead to the following for the equation of state, continuity equation and equations of motion:

$$\rho = 1 + \varepsilon P, \tag{1}$$

$$\frac{1}{r}\frac{\partial}{\partial r}(r\rho\bar{U}) + \frac{\partial}{\partial \bar{z}}(\rho V) = 0, \tag{2}$$

$$\alpha^3 Re\rho\left(\bar{U}\frac{\partial \bar{U}}{\partial r} + V\frac{\partial \bar{U}}{\partial \bar{z}}\right) = -8\frac{\partial P}{\partial r} + \alpha^2\frac{\partial}{\partial r}\left(\frac{1}{r}\frac{\partial}{\partial r}(r\bar{U})\right) + \alpha^4\frac{\partial^2 \bar{U}}{\partial \bar{z}^2} + \alpha^2\left(\chi + \frac{1}{3}\right)\left[\frac{\partial}{\partial r}\left(\frac{1}{r}\frac{\partial}{\partial r}(r\bar{U})\right) + \frac{\partial^2 V}{\partial r\partial \bar{z}}\right], \tag{3}$$

$$\alpha Re\rho\left(\bar{U}\frac{\partial V}{\partial r} + V\frac{\partial V}{\partial \bar{z}}\right) = -8\frac{\partial P}{\partial \bar{z}} + \frac{1}{r}\frac{\partial}{\partial r}\left(r\frac{\partial V}{\partial r}\right) + \alpha^2\frac{\partial^2 V}{\partial \bar{z}^2} + \alpha^2\left(\chi + \frac{1}{3}\right)\left[\frac{\partial}{\partial \bar{z}}\left(\frac{1}{r}\frac{\partial}{\partial r}(r\bar{U})\right) + \frac{\partial^2 V}{\partial \bar{z}^2}\right]. \tag{4}$$

The overbar indicates quantities re-scaled by the capillary aspect ratio: $\bar{z} = \alpha z$; $\bar{U} = U/\alpha$. Equations (1)–(4) contain the following dimensionless parameters:

$$\chi = \frac{\zeta}{\mu}, \quad \alpha = \frac{R}{L}, \quad Re = \frac{W}{\pi R\mu}, \quad \varepsilon = \frac{8\mu LW\kappa}{\rho_0\pi R^4} = \frac{8\gamma Ma^2}{\alpha Re},$$
$$\gamma = \frac{C_P}{C_V} \quad \text{and} \quad Ma = \frac{W}{\rho_0\pi R^2 c},$$

where $c^2 = \gamma(\partial P/\partial\rho)_T$ is the speed of sound. We consider subsonic flows so that $Ma < 1$. Note that both Re and Ma are based on the characteristic velocity and density at the capillary exit. Generally, for low-density, monatonic gases it is assumed that $\chi = 0$, but for dense gases and liquids, χ can be large (Karim & Rosenhead 1952).

Now we briefly discuss the previous studies on compressible viscous fluid flow in capillaries. In the analyses of Prud'home *et al.* (1986) and van den Berg *et al.* (1993*a*), the radial velocity and radial pressure gradient were assumed to be zero;

equations (2) and (4) with $\bar{U} = 0$ were solved using perturbation methods. Prud'homme *et al.* (1986) considered the flow of a monatomic ideal gas ($\rho \propto P$, $\chi = 0$) and found expressions for $V(r, \bar{z})$ and $P(\bar{z})$ as expansions in the parameters α and ε. van den Berg *et al.* (1993*a*) considered the flow of a fluid with an arbitrary equation of state and obtained a perturbation solution for $V(r)$ in terms of parameters involving $\alpha Re\varepsilon$ and $(\chi + 4/3)\alpha^2\varepsilon^2$. From (3), we see however that $\bar{U} = 0$ does not necessarily imply that the radial pressure gradient is zero; this fact was noted by van den Berg *et al.* (1993*a*). It is evident from (3) that a radially uniform pressure field is obtained for $\alpha Re \lesssim 1, \chi \lesssim 1$ if all terms order α^n for $n \geqslant 2$ are neglected – the so-called lubrication approximation (Batchelor 1967). In the analyses performed by Prud'homme *et al.* (1986) and van den Berg *et al.* (1993*a*), terms of order α^2 have been retained in (4), but neglected in (3); hence, they do not satisfy the compatibility condition for the equations of motion.

Velocity boundary conditions along the centreline and capillary wall are

$$\bar{U}(0, \bar{z}) = \frac{\partial V}{\partial r}(0, \bar{z}) = 0, \quad 0 \leqslant \bar{z} \leqslant 1, \tag{5a, b}$$

$$\bar{U}(1, \bar{z}) = V(1, \bar{z}) = 0, \quad 0 \leqslant \bar{z} \leqslant 1. \tag{6a, b}$$

In addition, we specify a reference pressure at the wall of the capillary exit as follows:

$$P(1, 1) = 0 \tag{7}$$

Equations (2)–(4) can also be expressed in terms of a stream function ψ defined by

$$\bar{U} = \frac{1}{r\rho}\frac{\partial \psi}{\partial \bar{z}}, \quad V = -\frac{1}{r\rho}\frac{\partial \psi}{\partial r}, \tag{8a, b}$$

and vorticity ω defined by

$$\omega = \alpha^2 \frac{\partial \bar{U}}{\partial \bar{z}} - \frac{\partial V}{\partial r}. \tag{9}$$

Using (2)–(4), (8) and (9), the pressure gradient can be expressed as

$$8\frac{\partial P}{\partial r} = \alpha^2 \frac{\partial \omega}{\partial \bar{z}} + \alpha^2\left(\gamma + \frac{4}{3}\right)\frac{\partial}{\partial r}\left(\frac{1}{r}\frac{\partial}{\partial r}(r\bar{U}) + \frac{\partial V}{\partial \bar{z}}\right) - \alpha^3 Re\left(\frac{1}{r}\frac{\partial \psi}{\partial \bar{z}}\frac{\partial \bar{U}}{\partial r} - \frac{1}{r}\frac{\partial \psi}{\partial r}\frac{\partial \bar{U}}{\partial \bar{z}}\right), \tag{10}$$

$$8\frac{\partial P}{\partial \bar{z}} = -\frac{1}{r}\frac{\partial}{\partial r}(r\omega) + \alpha^2\left(\gamma + \frac{4}{3}\right)\frac{\partial}{\partial \bar{z}}\left(\frac{1}{r}\frac{\partial}{\partial r}(r\bar{U}) + \frac{\partial V}{\partial \bar{z}}\right) - \alpha Re\left(\frac{1}{r}\frac{\partial \psi}{\partial \bar{z}}\frac{\partial V}{\partial r} - \frac{1}{r}\frac{\partial \psi}{\partial r}\frac{\partial V}{\partial \bar{z}}\right). \tag{11}$$

If (10) is differentiated with respect to $\bar{z}$, (11) with respect to r, and these results are combined using (8) and (9), the following form of the vorticity transport equation is obtained:

$$\frac{\partial}{\partial r}\left(\frac{1}{r}\frac{\partial}{\partial r}(r\omega)\right) + \alpha^2\frac{\partial^2 \omega}{\partial \bar{z}^2} = \alpha Re\left(\frac{1}{r}\frac{\partial \psi}{\partial \bar{z}}\frac{\partial \omega}{\partial r} - \frac{1}{r}\frac{\partial \psi}{\partial r}\frac{\partial \omega}{\partial \bar{z}} - \frac{\omega}{r^2}\frac{\partial \psi}{\partial \bar{z}}\right)$$
$$- \alpha Re\left[\omega\left(\bar{U}\frac{\partial \rho}{\partial r} + V\frac{\partial \rho}{\partial \bar{z}}\right) + \frac{\partial \rho}{\partial r}\left(\bar{U}\frac{\partial V}{\partial r} + V\frac{\partial V}{\partial \bar{z}}\right) - \alpha^2\frac{\partial \rho}{\partial \bar{z}}\left(\bar{U}\frac{\partial \bar{U}}{\partial r} + V\frac{\partial \bar{U}}{\partial \bar{z}}\right)\right]. \tag{12}$$

The vorticity transport equation for compressible *and* viscous fluids is rarely considered in fluid mechanics. The first line of (12) governs vorticity transport for

incompressible flow; the last term on the right-hand side represents the intensification of vorticity from vortex tube stretching (Batchelor 1967). The first term in the second line of (12) is vorticity intensification due to the dilation of vortex tubes. The second and third terms in the second line of (12) can be thought of as source terms from torques exerted on vortex tubes arising from fluid expansion.

Finally, if (8) is substituted in (9), we obtain

$$r\frac{\partial}{\partial r}\left(\frac{1}{r}\frac{\partial \psi}{\partial r}\right)+\alpha^2\frac{\partial^2\psi}{\partial \bar{z}^2}=\rho\omega r+\left(\alpha^2\bar{U}\frac{\partial \rho}{\partial \bar{z}}-V\frac{\partial \rho}{\partial r}\right)r. \tag{13}$$

It is interesting to note the effect compressibility has on the equations governing vorticity and stream function. Both (12) and (13) have an implicit dependence on P through ρ. Consequently, in contrast to constant-density flows, pressure is not eliminated by reformulating the governing equations in terms of vorticity and stream function. We will see however that the solution method developed in the next section is facilitated by considering the vorticity–stream function formulation.

The following set of boundary conditions can be derived from (5) and (6):

$$\psi(0,\bar{z})=\frac{1}{2},\quad \omega(0,\bar{z})=0,\quad 0\leqslant\bar{z}\leqslant 1, \tag{14a, b}$$

$$\frac{\partial\psi}{\partial r}(1,\bar{z})=\psi(1,\bar{z})=0,\quad \rho(1,\bar{z})\omega(1,\bar{z})=\frac{\partial^2\psi}{\partial r^2}(1,\bar{z}),\quad 0\leqslant\bar{z}\leqslant 1. \tag{15a, b, c}$$

The boundary condition in (14*a*) fixes the (dimensionless) mass flow rate at a value of one. The vorticity boundary condition at the capillary wall given in (15*c*) was derived using (15*a*) and (15*b*) in (13) (Vrentas, Duda & Bargeron 1967).

In order to solve (3) and (4) for $\bar{U}$ and V, or (12) and (13) for ω and ψ, which are both elliptic PDEs, boundary conditions are required at the capillary entrance and exit. The specification of boundary conditions at the entrance and exit to a flow domain is a delicate issue (Van Dyke 1970; Wilson 1971). The issue of inlet and outlet boundary conditions will be addressed later.

3. Perturbation solution

The equations governing the flow of a compressible Newtonian fluid in a capillary are nonlinear, and, consequently, it is not possible to find an exact analytical solution. The situation of interest is one involving a small departure from laminar flow of an incompressible liquid in capillary, which corresponds to a small value of the parameter ε. Based on this, we seek an approximate solution of the governing equations formulated in the previous section using perturbation methods. Before proceeding, it worthwhile to note that in previous analyses (Prud'home *et al.* 1986; van den Berg *et al.* 1993*a*), very different perturbation schemes were used. In both cases, the lubrication approximation is implicitly invoked since the radial pressure gradient was assumed negligible, yet the capillary aspect ratio α was used in the perturbation scheme. In the scheme used by van den Berg *et al.* (1993*a*), lumped perturbation parameters $\alpha Re\varepsilon$ and $(\chi+4/3)\alpha^2\varepsilon^2$ were used making it difficult to isolate the effects of compressibility, inertia and bulk viscosity. For this flow, compressibility induces inertial forces and volumetric deformations. Hence, it seems preferable to use a single perturbation parameter and allow the dimensionless parameters dictating these effects to arise in a natural way.

Writing the dependent variables as expansions in the perturbation parameter ε, we have

$$\rho = \rho^{(0)} + \varepsilon\rho^{(1)} + \varepsilon^2\rho^{(2)} + O(\varepsilon^3), \tag{16}$$
$$P = P^{(0)} + \varepsilon P^{(1)} + \varepsilon^2 P^{(2)} + O(\varepsilon^3), \tag{17}$$
$$\bar{U} = \bar{U}^{(0)} + \varepsilon\bar{U}^{(1)} + \varepsilon^2\bar{U}^{(2)} + O(\varepsilon^3), \tag{18}$$
$$V = V^{(0)} + \varepsilon V^{(1)} + \varepsilon^2 V^{(2)} + O(\varepsilon^3), \tag{19}$$
$$\psi = \psi^{(0)} + \varepsilon\psi^{(1)} + \varepsilon^2\psi^{(2)} + O(\varepsilon^3), \tag{20}$$
$$\omega = \omega^{(0)} + \varepsilon\omega^{(1)} + \varepsilon^2\omega^{(2)} + O(\varepsilon^3). \tag{21}$$

Here we employ a regular perturbation scheme substituting the expressions in (16)–(21) in the hydrodynamic equations and collecting terms of the same order in the perturbation parameter ε.

3.1. *Zero-order solution*

As noted in the previous section, it is convenient to consider the vorticity–stream function formulation for this flow. The equations governing the zero-order stream function $\psi^{(0)}$ defined by

$$\bar{U}^{(0)} = \frac{1}{r}\frac{\partial\psi^{(0)}}{\partial\bar{z}}, \quad V^{(0)} = -\frac{1}{r}\frac{\partial\psi^{(0)}}{\partial r}, \tag{22a, b}$$

and vorticity $\omega^{(0)}$

$$\omega^{(0)} = \alpha^2\frac{\partial\bar{U}^{(0)}}{\partial\bar{z}} - \frac{\partial V^{(0)}}{\partial r}, \tag{23}$$

are given by

$$\frac{\partial}{\partial r}\left(\frac{1}{r}\frac{\partial}{\partial r}\left(r\omega^{(0)}\right)\right) + \alpha^2\frac{\partial^2\omega^{(0)}}{\partial\bar{z}^2} = 0, \tag{24}$$
$$r\frac{\partial}{\partial r}\left(\frac{1}{r}\frac{\partial\psi^{(0)}}{\partial r}\right) + \alpha^2\frac{\partial^2\psi^{(0)}}{\partial\bar{z}^2} = \omega^{(0)}r. \tag{25}$$

The solutions of (24) and (25) subject to the boundary conditions

$$\psi^{(0)}(0,\bar{z}) = \tfrac{1}{2}, \quad \omega^{(0)}(0,\bar{z}) = 0, \tag{26a, b}$$

$$\psi^{(0)}(1,\bar{z}) = 0, \quad \omega^{(0)}(1,\bar{z}) = \frac{\partial^2\psi^{(0)}}{\partial r^2}(1,\bar{z}), \tag{27a, b}$$

are simply

$$\omega^{(0)} = 4r, \tag{28}$$
$$\psi^{(0)} = \frac{1}{2} - \left(1 - \frac{r^2}{2}\right)r^2. \tag{29}$$

The pressure gradient can be expressed as

$$8\frac{\mathrm{d}P^{(0)}}{\mathrm{d}\bar{z}} = -\frac{1}{r}\frac{\mathrm{d}}{\mathrm{d}r}\left(r\omega^{(0)}\right), \tag{30}$$

which is integrated with the condition

$$P^{(0)}(1) = 0. \tag{31}$$

Hence, from (28)–(31), we find the following for the zero-order axial velocity and pressure:

$$V^{(0)} = 2(1 - r^2), \tag{32}$$

$$P^{(0)} = 1 - \bar{z}. \tag{33}$$

Equations (32) and (33) correspond to the well-known solution for laminar flow of an incompressible Newtonian fluid in a capillary.

3.2. *First-order solution*

The equations governing the first-order stream function $\psi^{(1)}$ defined by

$$\bar{U}^{(1)} = \frac{1}{r}\frac{\partial \psi^{(1)}}{\partial \bar{z}}, \quad V^{(1)} = -\frac{1}{r}\frac{\partial \psi^{(1)}}{\partial r} - 2(1 - r^2)(1 - \bar{z}), \tag{34a, b}$$

and vorticity $\omega^{(1)}$

$$\omega^{(1)} = \alpha^2 \frac{\partial \bar{U}^{(1)}}{\partial \bar{z}} - \frac{\partial V^{(1)}}{\partial r}, \tag{35}$$

are given by

$$\frac{\partial}{\partial r}\left(\frac{1}{r}\frac{\partial}{\partial r}\left(r\omega^{(1)}\right)\right) + \alpha^2 \frac{\partial^2 \omega^{(1)}}{\partial \bar{z}^2} = 2\alpha Re(1 - r^2)\left(4r + \frac{\partial \omega^{(1)}}{\partial \bar{z}}\right), \tag{36}$$

$$r\frac{\partial}{\partial r}\left(\frac{1}{r}\frac{\partial \psi^{(1)}}{\partial r}\right) + \alpha^2 \frac{\partial^2 \psi^{(1)}}{\partial \bar{z}^2} = \left[\omega^{(1)} + 4r(1 - \bar{z})\right]r. \tag{37}$$

Equation (36) governing $\omega^{(1)}$ is a convection–diffusion equation with a source due to vortex tube dilation. Boundary conditions along the centreline and capillary wall for (36) and (37) are given by

$$\psi^{(1)}(0, \bar{z}) = \omega^{(1)}(0, \bar{z}) = 0, \quad 0 \leqslant \bar{z} \leqslant 1, \tag{38a, b}$$

$$\frac{\partial \psi^{(1)}}{\partial r}(1, \bar{z}) = \psi^{(1)}(1, \bar{z}) = 0, \quad \omega^{(1)}(1, \bar{z}) = \frac{\partial^2 \psi^{(1)}}{\partial r^2}(1, \bar{z}) - 4(1 - \bar{z}), \quad 0 \leqslant \bar{z} \leqslant 1. \tag{39a, b, c}$$

As noted above, we have not specified boundary conditions at the capillary entrance and exit. Here, we construct a solution by assuming simple functional forms for $\omega^{(1)}$ and $\psi^{(1)}$ that satisfy (36) and (37): $\omega^{(1)} = -4r(1 - \bar{z})$ plus a function of r, and $\psi^{(1)}$ is a function of r only. This procedure leads to solutions of (36)–(39) given by

$$\omega^{(1)} = -4r(1 - \bar{z}) - \tfrac{1}{3}\alpha\, Re\, r(3 - 6r^2 + 2r^4), \tag{40}$$

$$\psi^{(1)} = \tfrac{1}{72}\alpha Re r^2(1 - r^2)^2(4 - r^2). \tag{41}$$

The first-order pressure gradient can be written as

$$8\frac{\partial P^{(1)}}{\partial r} = \alpha^2 \frac{\partial \omega^{(1)}}{\partial \bar{z}} - 4\alpha^2\left(\frac{4}{3} + \chi\right)r, \tag{42}$$

$$8\frac{\partial P^{(1)}}{\partial \bar{z}} = -\frac{1}{r}\frac{\partial}{\partial r}\left(r\omega^{(1)}\right) - 4\alpha Re(1 - r^2)^2, \tag{43}$$

which is integrated subject to the condition

$$P^{(1)}(1, 1) = 0. \tag{44}$$

From (34) and (40)–(44), we obtain the following for the axial velocity and pressure:

$$V^{(1)} = 2(1-r^2)\big[-(1-\bar{z}) - \tfrac{1}{36}\alpha Re(2-7r^2+2r^4)\big], \tag{45}$$

$$P^{(1)} = -\tfrac{1}{2}(1-\bar{z})^2 + \tfrac{1}{4}\alpha Re(1-\bar{z}) + \tfrac{1}{4}\alpha^2\big(\tfrac{1}{3}+\chi\big)(1-r^2). \tag{46}$$

This analysis shows that to first order in ε, the radial velocity is zero, the axial velocity deviates from a parabolic distribution and the pressure field is not uniform in the radial direction.

3.3. *Second-order solution*

The equations governing the second-order stream function $\psi^{(2)}$ defined by

$$\bar{U}^{(2)} = \frac{1}{r}\frac{\partial \psi^{(2)}}{\partial \bar{z}}, \tag{47a}$$

$$V^{(2)} = -\frac{1}{r}\frac{\partial \psi^{(2)}}{\partial r} + 2(1-r^2)\left[\tfrac{3}{2}(1-\bar{z})^2 - \tfrac{1}{4}\alpha^2\left(\frac{1}{3}+\gamma\right)(1-r^2) - \tfrac{1}{36}\alpha Re(7+7r^2-2r^4)(1-\bar{z})\right], \tag{47b}$$

and vorticity $\omega^{(2)}$

$$\omega^{(2)} = \alpha^2\frac{\partial \bar{U}^{(2)}}{\partial \bar{z}} - \frac{\partial V^{(2)}}{\partial r}, \tag{48}$$

are given by

$$\frac{\partial}{\partial r}\left(\frac{1}{r}\frac{\partial}{\partial r}\big(r\omega^{(2)}\big)\right) + \alpha^2\frac{\partial^2\omega^{(2)}}{\partial \bar{z}^2} = 2\alpha Re(1-r^2)\left[\frac{\partial \omega^{(2)}}{\partial \bar{z}} - 24r(1-\bar{z}) - \tfrac{4}{9}\alpha Re\, r(2-16r^2+5r^4)\right], \tag{49}$$

$$r\frac{\partial}{\partial r}\left(\frac{1}{r}\frac{\partial \psi^{(2)}}{\partial r}\right) + \alpha^2\frac{\partial^2\psi^{(2)}}{\partial \bar{z}^2} = \big[\omega^{(2)} - 6r(1-\bar{z})^2 + 2\alpha^2\big(\tfrac{1}{3}+\chi\big)r(1-r^2) + \tfrac{2}{3}\alpha Re\, r^3(3-r^2)(1-\bar{z})\big]r. \tag{50}$$

Note that at second order, the radial convection and vortex tube stretching terms in (12) cancel. The source terms in (49) governing $\omega^{(2)}$ are due to axial convection of vorticity and vortex tube dilation. The boundary conditions along the centreline and capillary wall for (49) and (50) are

$$\psi^{(2)}(0,\bar{z}) = \omega^{(2)}(0,\bar{z}) = 0, \quad 0 \leqslant \bar{z} \leqslant 1, \tag{51a, b}$$

$$\frac{\partial \psi^{(2)}}{\partial r}(1,\bar{z}) = \psi^{(2)}(1,\bar{z}) = 0, \quad \omega^{(2)}(1,\bar{z}) = \frac{\partial^2\psi^{(2)}}{\partial r^2}(1,\bar{z}) + 6(1-\bar{z}) - \tfrac{4}{3}\alpha Re(1-\bar{z}), \quad 0 \leqslant \bar{z} \leqslant 1. \tag{52a, b, c}$$

As before, in the absence of a complete set of boundary conditions, we construct solutions by postulating the simplest expressions for $\omega^{(2)}$ and $\psi^{(2)}$ that satisfy (49)–(52). These are

$$\omega^{(2)} = 6r(1-\bar{z})^2 + \alpha^2 r\big(1-\tfrac{3}{2}r^2\big) - \tfrac{2}{3}\alpha^2\big(\tfrac{1}{3}+\gamma\big)r + 2\alpha Re\, r(1-3r^2+r^4)(1-\bar{z}) + \tfrac{1}{540}\alpha^2 Re^2 r(50-330r^2+540r^4-285r^6+42r^8), \tag{53}$$

$$\psi^{(2)} = -\tfrac{1}{24}\alpha^2\left[\tfrac{3}{2} + 2\left(\tfrac{1}{3}+\gamma\right)\right] r^2(1-r^2)^2 - \tfrac{1}{36}\alpha Re\, r^2(1-r^2)^2(4-r^2)(1-\bar{z}) - \frac{1}{43200}\alpha^2 Re^2\, r^2(1-r^2)^2(43-414r^2+229r^4-28r^6). \quad (54)$$

The second-order pressure gradient can be written as

$$8\frac{\partial P^{(2)}}{\partial r} = \alpha^2\frac{\partial \omega^{(2)}}{\partial \bar{z}} + 12\alpha^2\left(\tfrac{4}{3}+\gamma\right) r\left[(1-\bar{z}) + \tfrac{1}{18}\alpha Re\, r^2(3-r^2)\right], \quad (55)$$

$$8\frac{\partial P^{(2)}}{\partial \bar{z}} = -\frac{1}{r}\frac{\partial}{\partial r}\left(r\omega^{(2)}\right) + 6\alpha^2\left(\tfrac{4}{3}+\gamma\right)(1-r^2) + 12\alpha Re(1-r^2)^2(1-\bar{z}) - \tfrac{1}{9}\alpha^2 Re^2(1-r^2)^2(1+24r^2-7r^4), \quad (56)$$

which can be integrated subject to the condition

$$P^{(2)}(1,1) = 0. \quad (57)$$

From (47) and (53)–(56), we find following expressions for the second-order velocity and pressure:

$$\bar{U}^{(2)} = \tfrac{1}{36}\alpha Re\, r(1-r^2)^2(4-r^2), \quad (58)$$

$$V^{(2)} = 2(1-r^2)\left[\tfrac{3}{2}(1-\bar{z})^2 - \tfrac{1}{6}\alpha^2\left(\tfrac{1}{3}+\chi\right) + \tfrac{1}{16}\alpha^2(1-3r^2) - \tfrac{1}{12}\alpha Re(1+7r^2-2r^4) \times (1-\bar{z}) + \frac{1}{43200}\alpha^2 Re^2(43-957r^2+2343r^4-1257r^6+168r^8)\right], \quad (59)$$

$$P^{(2)} = \tfrac{1}{2}(1-\bar{z})^3 - \tfrac{1}{12}\alpha^2\left(\tfrac{1}{3}+\chi\right)(11-9r^2)(1-\bar{z}) - \tfrac{1}{2}\alpha Re(1-\bar{z})^2 - \tfrac{1}{2}\alpha^2(1-\bar{z}) + \tfrac{1}{27}\alpha^2 Re^2(1-\bar{z})^2 + \tfrac{1}{144}\alpha^3 Re(1-r^2)\left[(4-14r^2+4r^4) + \left(\tfrac{1}{3}+\chi\right)(7+7r^2-2r^4)\right]. \quad (60)$$

3.4. *Two-dimensional velocity and pressure fields*

We now combine the zero-, first- and second-order solutions derived above. The velocity and pressure fields are given by

$$U = \alpha\bar{U} = \tfrac{1}{36}\varepsilon^2\alpha^2 Re\, r(1-r^2)^2(4-r^2) + O(\varepsilon^3), \quad (61)$$

$$V = 2(1-r^2)\left[1 - \varepsilon(1-\bar{z}) + \tfrac{3}{2}\varepsilon^2(1-\bar{z})^2 - \tfrac{1}{36}\varepsilon\alpha Re(2-7r^2+2r^4) - \tfrac{1}{12}\varepsilon^2\alpha Re(1+7r^2-2r^4)(1-\bar{z}) - \tfrac{1}{6}\varepsilon^2\alpha^2\left(\tfrac{1}{3}+\gamma\right) + \tfrac{1}{16}\varepsilon^2\alpha^2(1-3r^2) + \frac{1}{43200}\varepsilon^2\alpha^2 Re^2(43-957r^2+2343r^4-1257r^6+168r^8)\right] + O(\varepsilon^3), \quad (62)$$

$$P = (1-\bar{z}) - \tfrac{1}{2}\varepsilon(1-\bar{z})^2 + \tfrac{1}{4}\varepsilon\alpha Re(1-\bar{z}) + \tfrac{1}{4}\varepsilon\alpha^2\left(\tfrac{1}{3}+\gamma\right)(1-r^2) + \tfrac{1}{2}\varepsilon^2(1-\bar{z})^3 - \tfrac{1}{2}\varepsilon^2\alpha^2(1-\bar{z}) - \tfrac{1}{12}\varepsilon^2\alpha^2\left(\tfrac{1}{3}+\chi\right)(11-9r^2)(1-\bar{z}) - \tfrac{1}{2}\varepsilon^2\alpha Re(1-\bar{z})^2 + \tfrac{1}{27}\varepsilon^2\alpha^2 Re^2(1-\bar{z})^2 + \tfrac{1}{144}\varepsilon^2\alpha^3 Re(1-r^2)\left[(4-14r^2+4r^4) + \left(\tfrac{1}{3}+\chi\right)(7+7r^2-2r^4)\right] + O(\varepsilon^3). \quad (63)$$

The density field to third order in ε is obtained by substitution of (63) in (1). It appears that (61) to (63) are the first two-dimensional velocity and pressure fields for capillary flow of compressible Newtonian fluids.

3.5. *Inlet and outlet boundary conditions*

As noted earlier, the velocity and pressure fields in (61)–(63) were obtained without specifying velocity boundary conditions on the closed domain at $\bar{z} = 0, 1$. In fact, (7), the boundary condition for pressure at the capillary wall, is the only boundary condition involving a particular axial position ($\bar{z} = 1$) within the capillary. One approach would be to assume slip tube flow at the capillary ends (Vrentas *et al.* 1967) so that velocity boundary conditions could be imposed at distances far from the capillary entrance and exit (Vrentas *et al.* 1967). However, this would result in mixed boundary conditions along the composite tube making it very difficult to find an analytical solution.

A solution obtained with an incomplete set of boundary conditions raises the question of its generality. One response to this question is that the velocity and pressure fields in (61)–(63) appear to be the simplest (non-trivial) solutions of the governing equations, but it is possible that more complex solutions exist. Schwartz (1987), in a two-dimensional analysis of compressible gas flow through a channel, avoided this issue by using a perturbation parameter involving the flow-direction coordinate normalized by a local wall pressure.

If boundary conditions at the inlet and outlet are to be specified, then the question is: what are these conditions? The answer is not at all obvious. The velocity fields given by (61) and (62) at $\bar{z} = 0, 1$ (see figures 3–5) show modest deviations from the incompressible flow case: $\bar{U} = 0$, $V = 2(1 - r^2)$. Similarly, the pressure field (see figure 3) given in (63) indicates that pressure is not uniform at the inlet and outlet. Unfortunately, published numerical solutions to this flow provide little guidance on this issue. For example, Guo & Wu (1997, 1998) only specify velocity boundary conditions $\bar{U} = 0$, $V = 2(1 - r^2)$, at the capillary inlet; Harley *et al.* (1995) only specify uniform pressures at the channel inlet and outlet.

For the flow of incompressible fluids, it is common to divide the capillary into entrance, fully developed flow, and exit regions. The solution for incompressible flow in the fully developed region (the zero-order solution in the present analysis) is obtained without specifying velocity boundary conditions at the inlet and outlet; it is implicitly assumed that this solution matches the velocity and pressure fields in the entrance and exit regions. While it is clear that a fully developed flow state does not exist for compressible flow, we assert that the same assumption holds. Indeed, this assumption is implicitly made in analyses based on the locally fully developed flow (lubrication) approximation. Hence, we argue the inlet and outlet velocity and pressure fields of the 'developing compressible flow' region match those in the transition regions at the capillary entrance and exit.

4. Approximate solutions

The two-dimensional solution presented in the previous section is valid for weakly compressible flow in a capillary. As noted in the introduction, other approximate solutions for this flow have been found. In this section, these approximate solutions are presented in order that comparisons with the solution obtained in the present study can be made.

4.1. *One-dimensional approximation*

It is common in the analysis of compressible flow to consider radially averaged forms of the conservation equations (Shapiro 1953). The radial average of a quantity $(\cdots)$

is defined as follows:

$$\langle(\cdots)\rangle = 2\int_0^1 (\cdots) r\,\mathrm{d}r. \tag{64}$$

Application of (64) to the continuity equation (2) and using (5*a*) and (6*a*) gives, after integration over $\bar{z}$ from 0 to 1,

$$\langle \rho V\rangle_1 = \langle \rho V\rangle_0 = \langle\rho\rangle\langle V\rangle + O(\varepsilon^2), \tag{65}$$

where the second equality follows from (1) and (63). Here, the subscripts 0 and 1 correspond to axial positions $\bar{z} = 0$ and $\bar{z} = 1$, respectively. Similarly, application of (64) to (4) and integration over $\bar{z}$ gives

$$\alpha Re[\langle\rho\rangle_1\langle V^2\rangle_1 - \langle\rho\rangle_0\langle V^2\rangle_0] = -8[\langle P\rangle_1 - \langle P\rangle_0] - \tfrac{1}{4} f Re + O(\varepsilon^2), \tag{66}$$

where f is the (Darcy) friction factor defined as

$$f = -\frac{8}{Re}\int_0^1 \frac{\partial V}{\partial r}(1,\bar{z})\,\mathrm{d}\bar{z}. \tag{67}$$

Now, if, as it is commonly assumed, we set $\langle V^2\rangle \simeq \langle V\rangle^2$ (Shapiro 1953), and (1), (62) and (63) are substituted in (66), we obtain the following expression for the one-dimensional model friction factor:

$$\frac{fRe}{32} = 1 - \tfrac{1}{2}\varepsilon + \tfrac{1}{8}\varepsilon\alpha Re + O(\varepsilon^2). \tag{68}$$

4.2. *Lubrication approximation*

As noted earlier, Prud'home *et al.* (1986) and van den Berg *et al.* (1993*a*) assumed that both the radial velocity and radial pressure gradient could be neglected (lubrication approximation) and solved (2) and (4). With $\bar{U} = 0$ and $P = P(\bar{z})$, (2) can be integrated to give:

$$V = \frac{E}{\rho} \tag{69}$$

where $E = E(r)$ and $\rho = \rho(\bar{z})$. Substitution of (69) in (4) gives

$$-\alpha Re\frac{1}{\rho}\frac{\mathrm{d}\rho}{\mathrm{d}\bar{z}}E^2 = -8\rho\frac{\mathrm{d}P}{\mathrm{d}\bar{z}} + \frac{1}{r}\frac{\mathrm{d}}{\mathrm{d}r}\left(r\frac{\mathrm{d}E}{\mathrm{d}r}\right) - \alpha^2\left(\frac{4}{3}+\chi\right)\frac{E}{\rho}\left[\frac{\mathrm{d}^2\rho}{\mathrm{d}\bar{z}^2} - \frac{2}{\rho}\left(\frac{\mathrm{d}\rho}{\mathrm{d}\bar{z}}\right)^2\right]. \tag{70}$$

Prud'home *et al.* (1986) solved (70) with $\rho \propto P$ and $\chi = 0$ by expanding E and P as double perturbation expansions in the parameters α and ε. The expression for axial velocity found by Prud'home *et al.* (1986) has a structure similar to (62) with respect to the grouping of the dimensionless parameters (ε, α, Re). However, in contrast to (63), the pressure field obtained by Prud'home *et al.* (1986) is independent of Re.

Here, we focus on the solution obtained by van den Berg *et al.* (1993*a*) who solved (70) using a somewhat different approach. The same approach has been adopted in more recent analyses of compressible flow in capillaries and channels (Zohar *et al.* 2002). In van den Berg *et al.* (1993*a*), (70) is integrated over the length of the capillary, fixing the pressure at both ends; an approximate expression for the last term in (70) is introduced since it cannot be integrated exactly. As shown in the perturbation solution developed in the present study, the pressure field is uniform in the radial direction for $\chi \lesssim 1$, $\alpha Re \lesssim 1$ only if $\alpha^2 \ll 1$. Based on this, we neglect the last term in (70) and integrate over the length of the capillary using (1) with $P(1) = 0$ and

$P(0) = \Delta P$, which gives

$$\alpha Re \ln[\rho(\Delta P)] E^2 = 8\bar{\rho}\Delta P + \frac{1}{r}\frac{\mathrm{d}}{\mathrm{d}r}\left(r\frac{\mathrm{d}E}{\mathrm{d}r}\right) \tag{71}$$

where $\bar{\rho}$ is defined as (van den Berg *et al.* 1993*a*)

$$\bar{\rho} = \frac{1}{\Delta P}\int_0^{\Delta P} \rho \, \mathrm{d}P. \tag{72}$$

Substituting $E = E^{(0)} + \alpha Re E^{(1)} + \cdots$ in (71) and solving the resulting system of equations (van den Berg *et al.* 1993*a*), the following expression for E is obtained:

$$\begin{aligned} E = 2(1-r^2)\bar{\rho}\Delta P \Bigg[& 1 - \tfrac{1}{36}\alpha Re \bar{\rho}\Delta P \ln[\rho(\Delta P)](11 - 7r^2 + 2r^4) \\ & - \frac{1}{14400}(\alpha Re)^2(\bar{\rho}\Delta P \ln[\rho(\Delta P)])^2(2457 - 1943r^2 - 957r^4 + 243r^6 - 32r^8)\Bigg] \\ & + O((\alpha Re)^3). \end{aligned} \tag{73}$$

The solution given in van den Berg *et al.* (1993*a*) is derived for an arbitrary equation of state $\rho(P)$. To facilitate comparison with the present work, we use the equation of state in (1) so that $\bar{\rho} = 1 + \varepsilon\Delta P/2$ and $\bar{\rho}\Delta P \ln[\rho(\Delta P)] = \varepsilon\Delta P^2[1 + \varepsilon^2\Delta P^2/12 + \cdots]$. Combining these results with (8*b*), (14*a*), (15*b*), (69) and (73), gives the following implicit expression for ΔP:

$$\begin{aligned} \Delta P &= 1 - \tfrac{1}{2}\varepsilon\Delta P^2 + \tfrac{1}{4}\varepsilon\alpha Re\Delta P^3 + \tfrac{1}{8}\varepsilon^2\alpha Re\Delta P^4 - \tfrac{73}{540}\varepsilon^2\alpha^2 Re^2\Delta P^5 + O(\varepsilon^3) \\ &\simeq 1 - \tfrac{1}{2}\varepsilon + \tfrac{1}{4}\varepsilon\alpha Re + \tfrac{1}{8}\varepsilon^2\alpha Re - \tfrac{73}{540}\varepsilon^2\alpha^2 Re^2. \end{aligned} \tag{74}$$

According to (69), the axial velocity is found by dividing $E(r)$ by $\rho(\bar{z})$. However, by integrating (70) over the length of the capillary, $\rho(\bar{z})$ cannot be determined; only the average density $\bar{\rho}$ defined in (72) is known. If we assume $V \simeq E/\bar{\rho}$ and use (73) and (74), we find the following expression for the axial velocity:

$$\begin{aligned} V \simeq 2(1-r^2)\Bigg[& 1 - \tfrac{1}{2}\varepsilon - \tfrac{1}{36}\varepsilon\alpha Re(2 - 7r^2 + 2r^4) + \tfrac{1}{24}\varepsilon^2\alpha Re(14 - 7r^2 + 2r^4) \\ & - \frac{1}{43200}\varepsilon^2\alpha^2 Re^2(8369 - 471r^2 - 1071r^4 + 729r^6 - 96r^8)\Bigg]. \end{aligned} \tag{75}$$

Expressions for axial velocity from the lubrication approximation model (75) and two-dimensional model (62) with $\chi \lesssim 1$ and $\alpha^2 \ll 1$ are in agreement up to first order in ε. This is not surprising since the pressure field is uniform and radial velocity is zero to first order in ε for this case. However, significant deviations between (62) and (75) are apparent at second order in ε.

In the creeping flow limit where $\alpha Re \ll 1$, it is possible to find an analytical solution for the lubrication approximation model. For $\chi \lesssim 1$, $\alpha^2 \ll 1$ and $\alpha Re \ll 1$, (12) and (13) simplify to

$$\frac{\partial}{\partial r}\left(\frac{1}{r}\frac{\partial}{\partial r}(r\omega)\right) = 0, \tag{76}$$

$$\frac{\partial}{\partial r}\left(\frac{1}{r}\frac{\partial \psi}{\partial r}\right) = \rho\omega. \tag{77}$$

Integration of (76) and (77) subject to the boundary conditions in (14) and (15) gives

$$\omega = \frac{4}{\rho} r, \tag{78}$$

$$\psi = \frac{1}{2} - \left(1 - \frac{r^2}{2}\right) r^2. \tag{79}$$

From (11), the pressure gradient for $\chi \lesssim 1$, $\alpha^2 \ll 1$ and $\alpha Re \ll 1$ is given by

$$8 \frac{\mathrm{d}P}{\mathrm{d}\bar{z}} = -\frac{1}{r} \frac{\partial}{\partial r}(r\omega) \tag{80}$$

which, when integrated subject to (7), gives

$$P = \frac{\sqrt{1 + 2\varepsilon(1 - \bar{z})} - 1}{\varepsilon} = (1 - \bar{z}) - \tfrac{1}{2}\varepsilon(1 - \bar{z})^2 + \tfrac{1}{2}\varepsilon^2(1 - \bar{z})^3 + O(\varepsilon^3). \tag{81}$$

From (1), (8), (79) and (81), we find $\bar{U} = 0$ and

$$V = \frac{2}{\rho}(1 - r^2) = 2(1 - r^2)\left[1 - (1 - \bar{z})\varepsilon + \tfrac{3}{2}(1 - \bar{z})^2\varepsilon^2 + O(\varepsilon^3)\right]. \tag{82}$$

If the expression for P is expanded as a power series to second order in ε, as shown in (81), the second-order result agrees with the exact expression for $\varepsilon \lesssim 0.25$. As expected, we find agreement between (62) and (82) and between (63) and (81) for $\chi \lesssim 1$, $\alpha Re \ll 1$ and $\alpha^2 \ll 1$.

5. Results and discussion

The velocity and pressure fields given in (61)–(63) appear to be the first two-dimensional, analytical solutions for capillary flow of compressible Newtonian fluids. In contrast to previous analyses (Prud'home *et al.* 1986; van den Berg *et al.* 1993*a*), we find a non-zero radial velocity and non-zero radial pressure gradient. The axial velocity deviates from a parabolic radial dependence at first order in ε due to fluid inertia. At second order in ε, bulk viscosity leads to a reduction of the axial velocity, but does not affect its distribution. The flattening of the axial velocity profile with increasing $\varepsilon\alpha Re$ predicted by (62) is consistent with the numerical results of Guo & Wu (1997, 1998). The expression for the pressure field in (63) shows radial dependence at first order in ε due to bulk viscosity and at second order in ε due to bulk viscosity and inertia. It is clear from (63) that the lubrication approximation, which implies a radially uniform pressure, is valid for $\chi \lesssim 1$, $\alpha Re \lesssim 1$ only for long capillaries where $\alpha^2 \ll 1$. Unfortunately, the numerical results presented by Guo & Wu (1997, 1998) do not include radial velocity or radial pressure variations (if they were observed).

In the absence of comparable velocity and pressure fields from analytical and numerical solutions for compressible flow in capillaries, we briefly discuss results from studies of compressible flow in channels. Schwartz (1987) obtained a two-dimensional perturbation solution for the flow of a compressible gas through a channel. These velocity fields are consistent with those found here in that the transverse velocity was order $\varepsilon^2\alpha^2 Re$, as in (61); deviations from a parabolic axial velocity were order $\varepsilon\alpha Re$, as in (62). Harley *et al.* (1995) presented numerical solutions for compressible channel flow that displayed both transverse velocity and pressure gradient. It is important to note that these flow features, which are consistent with those reported in this study, were observed by imposing uniform pressures at the capillary entrance and exit (Harley *et al.* 1995).

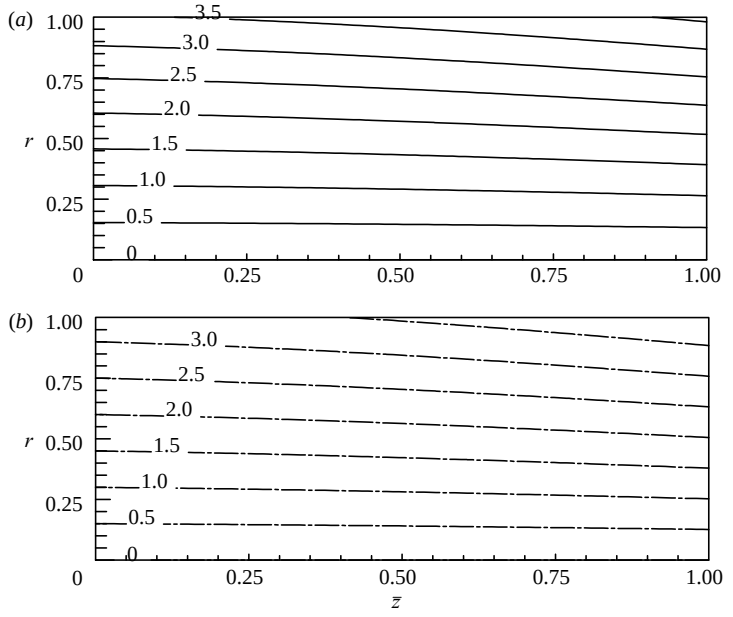

FIGURE 2. Vorticity field contours for $\varepsilon = 0.25$ from (83): (*a*) solid lines for $\alpha Re = 1$; $\alpha^2(1/3+\chi) \ll 1$; (*b*) dashed-dot lines for $\alpha Re \ll 1$; $\alpha^2(1/3+\chi) = 1$.

5.1. *Vorticity, velocity and pressure fields*

From the expressions given in (61)–(63), it is clear that in addition to the compressibility parameter ε, the velocity and pressure fields are influenced by αRe and $\alpha^2(1/3+\chi)$. Bulk viscosity data are scarce, but for ordinary liquids $1 \lesssim \chi \lesssim 10^2$ (Karim & Rosenhead 1952), and for gases $\chi \lesssim 1$. Since $\alpha \lesssim 1/10$, for gas flows it is clear that $\alpha^2(1/3+\chi) \ll 1$; for liquid flows in short capillaries, we use $\alpha^2(1/3+\chi) = 1$ as an upper bound. Based on a comparison of the exact expression and series expansion in (81), the compressibility parameter is limited to values $\varepsilon \leqslant 0.25$. In addition, for laminar flows $Re \lesssim 10^3$ so that we are restricted to $\alpha Re \lesssim 10^2$. Finally, since we are considering subsonic flows $Ma = \sqrt{\varepsilon \alpha Re/\gamma 8} < 1$.

It is instructive to examine the effects of compressibility on vorticity. From the perturbation solution presented in the previous section, the vorticity field to second order is given by

$$\omega = 4r\big[1-\varepsilon(1-\bar{z}) - \tfrac{1}{12}\varepsilon\alpha Re(3-6r^2+2r^4) + \tfrac{3}{2}\varepsilon^2(1-\bar{z})^2 + \tfrac{1}{4}\varepsilon^2\alpha^2\big(1-\tfrac{3}{2}r^2\big) - \tfrac{1}{6}\varepsilon^2\alpha^2\big(\tfrac{1}{3}+\gamma\big) + \tfrac{1}{2}\varepsilon^2\alpha Re(1-3r^2+2r^4)(1-\bar{z}) + \tfrac{1}{2160}\varepsilon^2\alpha^2 Re^2(50-330r^2 + 540r^4 - 285r^6 + 42r^8)\big] + O(\varepsilon^3). \tag{83}$$

For incompressible flow, the radial diffusion of vorticity towards the centre of the capillary is exactly balanced by the rate at which it is generated at the capillary wall. For compressible flow, density decreases while axial velocity increases (so that mass flow rate is constant) from the capillary entrance to the capillary exit. Hence, the vorticity generated at the capillary wall increases along the capillary. The axial gradient in vorticity gives rise to diffusion of vorticity towards the capillary entrance and convection of vorticity towards the capillary exit. Vorticity contours for $\varepsilon = 0.25$ with $\alpha Re = 1$, $\alpha^2(1/3+\chi) \ll 1$ and $\alpha^2(1/3+\chi) = 1$, $\alpha Re \ll 1$ are shown in figures 2(*a*) and 2(*b*). In both cases, fluid compressibility causes vorticity tubes to expand and

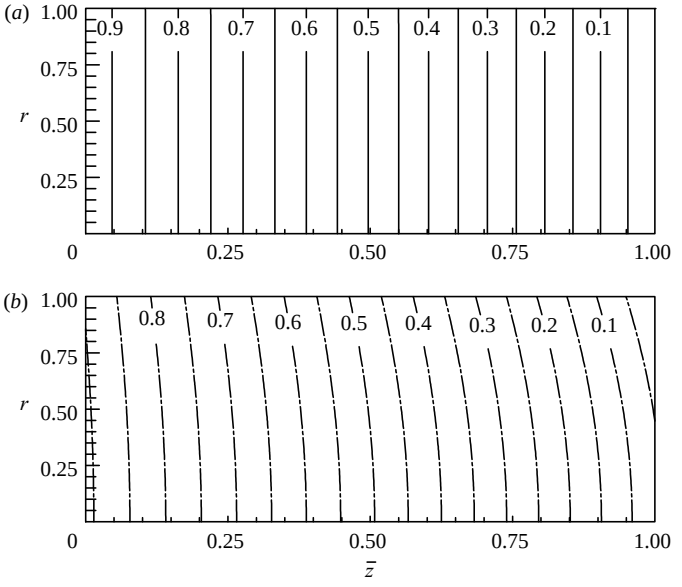

FIGURE 3. Pressure field contours for $\varepsilon = 0.25$ from (63): (*a*) solid lines for $\alpha Re = 1$; $\alpha^2(1/3 + \chi) \ll 1$; (*b*) dashed-dot lines for $\alpha Re \ll 1$; $\alpha^2(1/3 + \chi) = 1$.

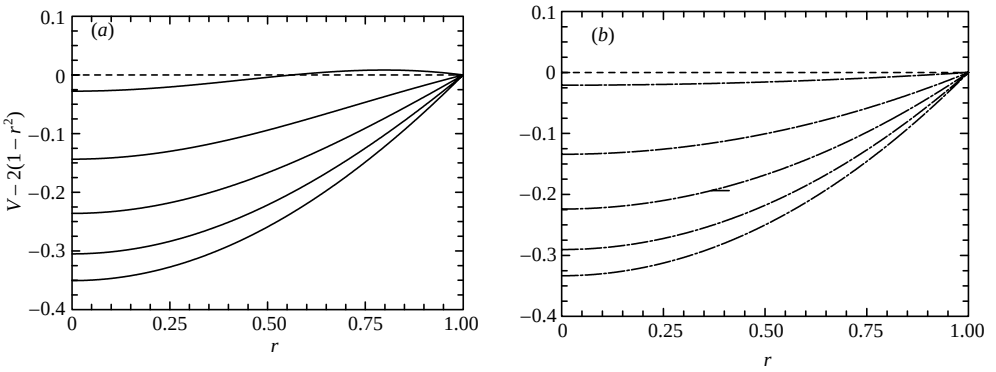

FIGURE 4. Axial velocity field deviation from incompressible flow: (*a*) from (62) for $\varepsilon = 0.25$, $\alpha Re = 1$, $\alpha^2(1/3 + \chi) \ll 1$ (*b*) $\alpha Re \ll 1$, $\alpha^2(1/3 + x) = 1$ at various axial positions: $\bar{z} = 0$, 0.25, 0.5, 0.75, 1.0 (bottom to top).

stretch near the capillary wall, moving towards the capillary entrance. For $\alpha Re = 1$, axial convection of vorticity concentrates vorticity near the capillary wall.

Pressure contours predicted by (63) are shown in figure 3 for the same cases shown in figure 2. Deviations from the incompressible case, for which pressure contours are equally spaced vertical lines, are evident in both cases. Although the pressure contours for $\alpha Re = 1$, $\alpha^2(1/3 + \chi) \ll 1$ appear to be vertical lines, a small and negative radial pressure gradient is predicted by (63) for this case. The pressure contours for $\alpha^2(1/3 + \chi) = 1$, $\alpha Re \ll 1$ show an appreciable radial pressure gradient resulting from bulk viscosity.

Figures 4(*a*) and 4(*b*) show the axial velocity field predicted by (62) for $\varepsilon = 0.25$. For $\alpha Re = 1$ shown in figure 4(*a*), fluid inertia ($\alpha Re = 1$) causes a pronounced flattening of the axial velocity profile from its parabolic shape as the fluid passes

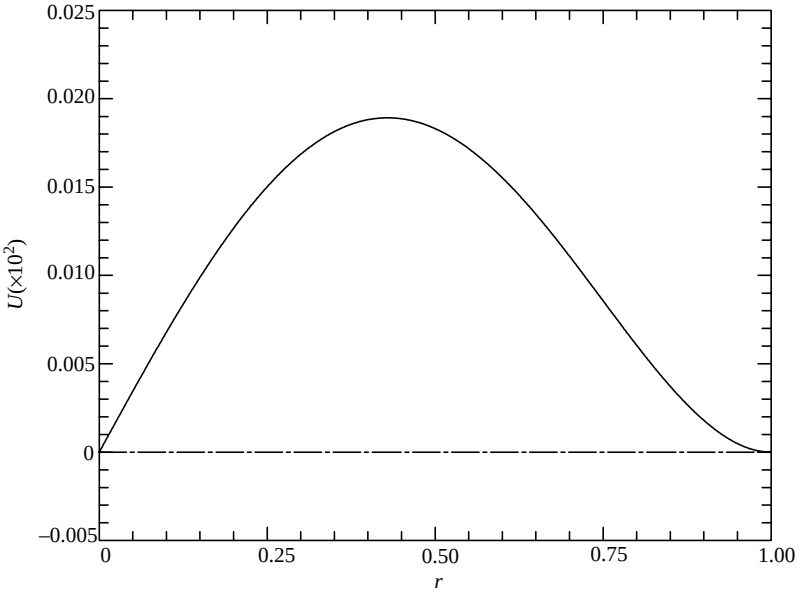

FIGURE 5. Radial velocity field for $\varepsilon = 0.25$ and $\alpha = 1/10$ from (61): solid line for $\alpha Re = 1$; $\alpha^2(1/3 + \chi) \ll 1$; dashed-dot line for $\alpha Re \ll 1$; $\alpha^2(1/3 + \chi) = 1$.

through the capillary. This behaviour is consistent with numerical results obtained by Guo & Wu (1997, 1998). For the case where $\alpha^2(1/3 + \chi) = 1$ (figure 4*b*), the effect of bulk viscosity is small and the axial velocity distribution remains parabolic.

Figure 5 shows the radial velocity field predicted by (61) for $\varepsilon = 0.25$. For $\alpha Re = 1$ and $\alpha = 1/10$, U is positive indicating a small radial flow towards the capillary wall. The radial flow arises from simple mass conservation and the coupling between inertia and compressibility. As fluid passes through the capillary, fluid inertia leads to a flattening of the axial velocity and compressibility leads to a reduction in density. The coupling of these two effects, through the $\rho\omega$ term in (13), induces a radial velocity at second order in ε. The small radial flow induces a small radial pressure gradient. In the absence of inertia, the velocity field remains parabolic and radial flow is not required to satisfy mass conservation. The relatively large radial pressure gradient for $\alpha^2(1/3 + \chi) = 1$ shown in figure 3(*b*) is balanced by the isotropic stresses induced by a large bulk viscosity.

5.2. *Friction factor and pressure drop*

The friction factor for the two-dimensional analysis is obtained by substitution of (62) in (67), which gives

$$\frac{f\,Re}{32} = 1 - \left[\tfrac{1}{2} - \tfrac{1}{12}\alpha Re\right]\varepsilon + \left[\tfrac{1}{2} - \tfrac{1}{8}\alpha^2 - \tfrac{1}{6}\alpha^2\left(\chi + \tfrac{1}{3}\right) - \tfrac{1}{4}\alpha Re + \tfrac{17}{2160}\alpha^2 Re^2\right]\varepsilon^2 + O(\varepsilon^3). \tag{84}$$

Comparison of (68) and (84) shows that the one-dimensional model over-predicts the effect of inertia; this error is due to the approximation $\langle V^2\rangle \simeq \langle V\rangle^2$. For $\varepsilon = 0.1$, $\alpha Re \simeq 10$, the one-dimensional model over-predicts the friction factor by roughly 10 %.

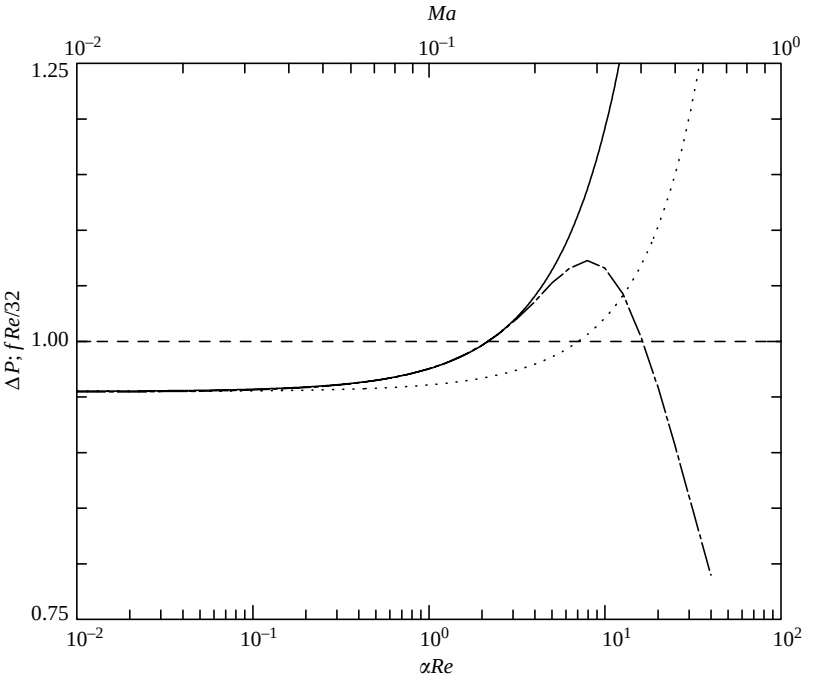

FIGURE 6. Comparison of pressure drops from different analyses for $\varepsilon = 0.1$. Two-dimensional model (86): solid line for $\alpha^2(1/3 + \chi) \ll 1$; lubrication approximation model (74): dashed-dot line. Also shown by the dotted line is the friction factor prediction for the two-dimensional model (84).

Viscosity measurements are often made using capillaries by measuring the pressure drop for a given flow rate, or vice versa for a capillary of known dimensions. The pressure drop is obtained from the pressures measured in fluid reservoirs at the entrance and exit of the capillary. Hence, the measured pressure reflects the difference in total stress at the ends of the capillary

$$\Delta P = \langle P(r,0)\rangle - \langle P(r,1)\rangle - \frac{\alpha^2}{8}\left(\tfrac{4}{3} + \chi\right)\left[\left\langle \frac{\partial V}{\partial \bar{z}}(r,0)\right\rangle - \left\langle \frac{\partial V}{\partial \bar{z}}(r,1)\right\rangle\right]. \quad (85)$$

Substitution of (62) and (63) in (85) gives

$$\Delta P = 1 - \left[\tfrac{1}{2} - \tfrac{1}{4}\alpha Re\right]\varepsilon + \left[\tfrac{1}{2} - \tfrac{1}{8}\alpha^2 - \tfrac{1}{6}\alpha^2\left(\tfrac{1}{3} + \chi\right) - \tfrac{1}{2}\alpha Re + \tfrac{1}{27}\alpha^2 Re^2\right]\varepsilon^2 + O(\varepsilon^3). \quad (86)$$

Equation (86) gives the pressure drop for capillary flow of compressible Newtonian fluids. The first term in (86) is the dimensionless form of the Hagen–Poiseuille equation, and the terms that follow give corrections due to fluid compressibility. In the absence of inertia and bulk viscosity effects, compressibility decreases the pressure drop. This is easily explained by the reduction in axial velocity, and hence shear stress, to compensate for the increase in density towards the capillary entrance. A large bulk viscosity further reduces the pressure drop, which is due to a small reduction in the axial velocity. Inertia, which results from fluid acceleration along the capillary, leads to a pronounced increase in pressure drop.

The pressure drop prediction from the two-dimensional model (86) is plotted in figure 6 for $\varepsilon = 0.1$ with α^2 and $\alpha^2(1/3 + \chi)$ terms neglected. The pressure drop for compressible flow is constant and reduced by approximately 5 % for $\alpha Re < 0.1$, or

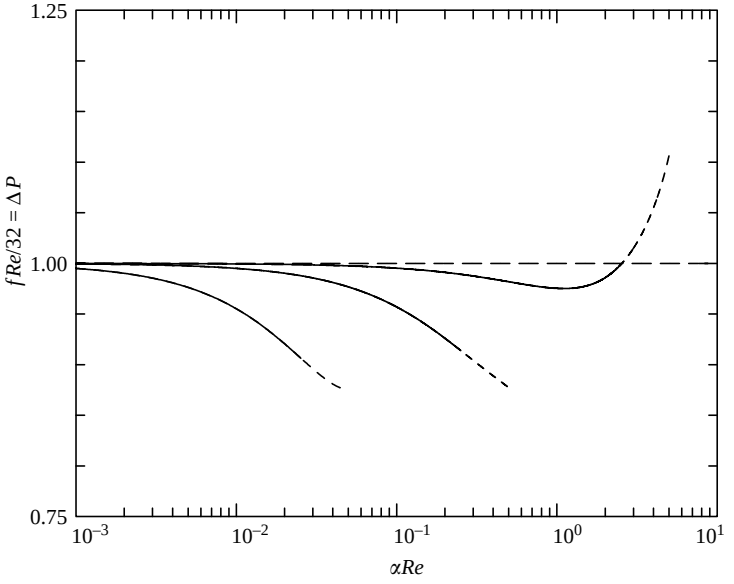

FIGURE 7. Friction factor based on pressure drop from (87) for different values of $\alpha^2 B = 0.1$, 1.0, 10 (bottom to top). Solid curves are drawn for values of αRe such that $\varepsilon \leqslant 0.25$.

$Ma < 0.03$. For $\alpha Re \gtrsim 1$ ($Ma \gtrsim 0.1$), the pressure drop increases dramatically above the incompressible value. Also shown in figure 7 is the pressure drop prediction for the lubrication approximation model, which was obtained by numerically solving (74) for ΔP. It is clear from figure 6 that the lubrication approximation model drastically under-predicts the pressure drop for $\alpha Re \gtrsim 3$.

It is common to define the friction factor in terms of pressure drop, rather than a drag force as in (67). For incompressible flow in a capillary, the results are identical: $fRe/32 = 1$. For compressible flow, $fRe/32 = \Delta P$, where ΔP is given by (86). Although similar, (84) and (86) differ by the numerical factors for the inertial (αRe) terms, which are significantly larger in (86) than in (84). These two friction factors are compared in figure 6 and clearly demonstrate that the effect of inertia on pressure drop is significantly larger than on drag force for compressible flow in capillaries.

As noted in the introduction, flows of gases and liquids in micro-capillaries commonly show deviations from the Hagen–Poiseuille equation. In most cases, the pressure drop is imposed and the resulting flow rate is measured. Hence, for a given set of experiments, the compressibility parameter ε is not constant. It is easy to show that $\varepsilon = \alpha Re/\alpha^2 B$ where

$$\alpha^2 B = \frac{\rho_0 R^4}{8\kappa\mu^2 L^2}$$

is a parameter that depends only on fluid properties and dimensions of the capillary. Hence, the expression for friction factor (or pressure drop) given in (86) can be written as

$$\frac{fRe}{32} = \Delta P = 1 - \frac{1}{2}\frac{\alpha Re}{\alpha^2 B} + \frac{1}{2}\frac{(\alpha Re)^2}{\alpha^2 B} + \frac{1}{4}\frac{(\alpha Re)^2}{(\alpha^2 B)^2} - \frac{1}{2}\frac{(\alpha Re)^3}{(\alpha^2 B)^2} + \frac{1}{27}\frac{(\alpha Re)^4}{(\alpha^2 B)^2} + \cdots, \quad (87)$$

where α^2 and $\alpha^2(1/3 + \chi)$ terms have been neglected. The friction factor (based on pressure drop) from (87) versus flow rate (αRe) is shown in figure 7; the solid

curves are drawn for values of αRe such that $\varepsilon \leqslant 0.25$. Values of the parameter $\alpha^2 B$ correspond to gas (<1) and liquid flow (>1) in a long ($\alpha = 10^{-3}$) micro-capillary ($R = 25\,\mu\text{m}$). As shown in figure 7, for $\alpha Re < 1$ and $\alpha^2 B \leqslant 1$, the friction factor is from zero to 10 % smaller than the value for incompressible flow. This is consistent with a large number of experiments on gas flows in micro-capillaries and channels (Papautsky *et al.* 2001). The predicted decrease in friction factor with decreasing capillary radius R and increasing Re has also been reported by Araki *et al.* (2000) for gas flows in micro-capillaries. The predicted increase in friction factor for $\alpha Re > 1$ and $\alpha^2 B = 10$ is consistent with the observations of Li, Du & Guo (2003) for water flows through micro-capillaries.

6. Conclusions

A two-dimensional solution for laminar flow of compressible Newtonian fluids in capillaries has been obtained. This solution, obtained using standard perturbation methods on the vorticity–stream function form of the governing hydrodynamics equations, predicts both a non-zero radial velocity and non-zero radial pressure gradient. These features of the velocity and pressure fields were neglected in previous analyses of this flow.

The effects of fluid inertia and bulk viscosity were examined and found to produce qualitatively different velocity and pressure fields. Fluid inertia has a significant effect on the axial velocity distribution and is responsible for the radial velocity. Bulk viscosity leads to a radial pressure gradient, but has little effect on the velocity field. Expressions for pressure drop and friction factor have been derived from the two-dimensional analysis. For slow flows ($\alpha Re \lesssim 1$, $Ma \gtrsim 0.1$), compressibility reduces pressure drop; for subsonic, high-speed flows ($\alpha Re > 1$, $0.1 < Ma < 1$), pressure drop increases dramatically. These trends are consistent with reported experimentals tudies on flows in micro-tubes and channels. Results from the two- dimensional analysis have been compared to results obtained using the one-dimensional and lubrication approximations. Deviations from the two-dimensional solution are observed at first order for the one-dimensional and at second order for lubrication approximation solutions. Friction factor and pressure drop predictions from the lubrication approximation model show significant deviations from those obtained with the two-dimensional solution when inertial effects become important.

The perturbation solution presented here represents an important advance in the analysis of compressible viscous fluid flow through capillaries. The approach used to obtain this solution could easily be applied to channels flows and to flows of rarified gases where slip is important. The study has also revealed the need for detailed numerical solutions of this flow, which, if available, would provide important insight into the range of validity of perturbation solutions.

This paper is dedicated to Dr Ernest R. Venerus on the occasion of his retirement after 40 years of dedicated service from Knolls Atomic Power Laboratory, Schenectady, New York. The author acknowledges useful discussions on this analysis with Professor J. S. Vrentas and the comments of an anonymous reviewer.

Appendix

The analysis presented above for the capillary flow of a compressible Newtonian fluid is based on the assumption that the flow is isothermal. The same assumption

was made by Prud'home *et al.* (1986), who performed an approximate analysis, and by van den Berg, ten Seldam & van der Gulik (1993*b*), who considered thermal effects in a separate study. So that we may examine thermal effects on compressible flow, we make several additional assumptions. First, we assume the fluid enters the capillary with uniform temperature T_0 and that the capillary wall is at a constant temperature T_0. It is assumed that the fluid is thermally simple so that conduction is described by Fourier's law with constant thermal conductivity k and the specific internal energy can be expressed in terms of density, temperature and constant specific heat C_P. We also assume that viscosity μ and bulk viscosity ζ are independent of temperature. Finally, we assume that the fluid density is a linear function of temperature with thermal expansivity β.

The continuity equation and equations of motion are the same as those given in (2), (3) and (4). If temperature T_0 is scaled by the temperature rise associated with viscous dissipation, $\mu W^2/k\pi^2R^4\rho_0^2$, the equation of state and thermal energy equation can be written as

$$\rho = 1 + \varepsilon P - \varepsilon_T T, \tag{A 1}$$

$$\begin{aligned}\alpha Pe\rho\left(\bar{U}\frac{\partial T}{\partial r} + V\frac{\partial T}{\partial \bar{z}}\right) &= \frac{1}{r}\frac{\partial}{\partial r}\left(r\frac{\partial T}{\partial r}\right) + \alpha^2\frac{\partial^2 T}{\partial \bar{z}^2} + 8\left(\varepsilon_T T + \lambda\right)\left(\bar{U}\frac{\partial P}{\partial r} + V\frac{\partial P}{\partial \bar{z}}\right)\\ &+ \left(\frac{\partial V}{\partial r}\right)^2 + \alpha^2\left(2\left[\left(\frac{\partial \bar{U}}{\partial r}\right)^2 + \left(\frac{\bar{U}}{r}\right)^2 + \left(\frac{\partial V}{\partial \bar{z}}\right)^2 + \left(\frac{\partial \bar{U}}{\partial \bar{z}}\frac{\partial V}{\partial r}\right)\right] + \alpha^2\left(\frac{\partial \bar{U}}{\partial \bar{z}}\right)^2\right.\\ &\left. + \left(\chi - \frac{2}{3}\right)\left[\frac{1}{r}\frac{\partial}{\partial r}(r\bar{U}) + \frac{\partial V}{\partial \bar{z}}\right]^2\right)\end{aligned} \tag{A 2}$$

which contain three dimensionless parameters:

$$\lambda = \beta T_0, \quad Pe = \frac{C_P W}{\pi R k}, \quad \varepsilon_T = \frac{\mu W^2 \beta}{k\rho_0^2\pi^2 R^4}.$$

Temperature boundary conditions for (A2) are given by

$$\frac{\partial T}{\partial r}(0, \bar{z}) = T(1, \bar{z}) = 0, \quad 0 \leqslant \bar{z} \leqslant 1, \tag{A 3a, b}$$

$$T(r, 0) = 0, \quad 0 \leqslant r \leqslant 1. \tag{A 4}$$

The dependent variables can be written as expansions in two perturbation parameters ε and ε_T. For $Pe \gg 1$, the equation governing the zero-order temperature field $T^{(0)}$ is

$$(1 - r^2)\frac{\partial T^{(0)}}{\partial \xi} = \frac{1}{r}\frac{\partial}{\partial r}\left(r\frac{\partial T^{(0)}}{\partial r}\right) + 16[r^2 - \lambda(1 - r^2)] \tag{A 5}$$

where $\xi = \bar{z}/Pe$. The boundary conditions and initial condition for (A5) can be written as

$$\frac{\partial T^{(0)}}{\partial r}(0, \xi) = T^{(0)}(1, \xi) = 0, \quad 0 \leqslant \xi < \infty, \tag{A 6a, b}$$

$$T^{(0)}(r, 0) = 0, \quad 0 \leqslant r \leqslant 1. \tag{A 7}$$

The set of equations given in (A 5)–(A 7) is similar to the problem considered by van den Berg *et al.* (1993*b*). From (A 5), we see that the viscous dissipationand expansion

terms tend to cancel each other, depending on the value of λ. For liquids and gases away from their critical point, this parameter is in the range $0.1 \lesssim \lambda \lesssim 1$.

Temperature profiles $T^{(0)}(r, \xi)$ for a range of λ values have been computed by van den Berg *et al.* (1993*b*). $T^{(0)} > 0$ near the capillary wall where viscous heating dominates expansion cooling; $T^{(0)} < 0$ near the centre of the capillary where expansion cooling dominates viscous heating. For $\lambda \lesssim 0.42$, the radial-average temperature $\langle T^{(0)} \rangle$ monotonically increases with ξ, and for $0.5 < \lambda \leqslant 1$, $\langle T^{(0)} \rangle$ monotonically decreases with ξ. For $Pe \gg 1$, however, we need only to consider the temperature field for $\xi \ll 1$, where $\langle T^{(0)} \rangle \sim 16(\frac{1}{2} - \lambda)\xi$ and $|T^{(0)} - \langle T^{(0)} \rangle| \lesssim 0.1$ for $0 \leqslant \lambda \leqslant 1$. This means that over the length of the capillary ($0 \leqslant \xi \leqslant 1/Pe$), the temperature field does not deviate significantly from its value at the entrance. Hence, for $\varepsilon_T \ll 1$ and $Pe \gg 1$, the flow is effectively *isothermal*.

REFERENCES

Araki, T., Fujimoto, R., Kim, M. S., Inaoka, K. & Suzuki, K. 2000 Gas flow characteristics in microtubes. *JSME Intl J.* B **43**, 634–639.

Batchelor, G. K. 1967 *An Introduction to Fluid Dynamics*. Cambridge University Press.

van den Berg, H. R., ten Seldam, C. A. & van der Gulik, P. S. 1993*a* Compressible laminar flow in a capillary. *J. Fluid Mech.* **246**, 1–20.

van den Berg, H. R., ten Seldam, C. A. & van der Gulik, P. S. 1993*b* Thermal effects in compressible viscous flow in a capillary. *Intl J. Thermophys.* **14**, 865–892.

Beskok, A., Karniadakis, G. E. & Trimmer, W. 1996 Rarefaction and compressibility effects in gas microflows. *J. Fluids Engng* **118**, 448–456.

Gad-el-Hak, M. 1999 The fluid mechanics of microdevices – The Freeman Scholar Lecture. *J. Fluids Engng* **121**, 5–33.

Guo, Z. Y. & Wu, X. B. 1997 Compressibility effect on the gas flow and heat transfer in a microtube. *Intl J. Heat Mass Transfer* **40**, 3251–3254.

Guo, Z. Y. & Wu, X. B. 1998 Further study on compressibility effects on the gas flow and heat transfer in a microtube. *Microscale Thermophys. Engng* **2**, 111–120.

Hagen, G. 1839 Über die Bewegung des Wassers in egen zylinderschen Rohren. *Pogg. Ann. Phys. Chem.* **46**, 423–442.

Hagenbach, E. 1860 Über die Bestimmung der Zähigkeit einer Flüssigkeit durch den Ausfluss aus Rohren. *Pogg. Ann. Phys. Chem.* **108**, 385–426.

Harley, J. C., Huang, Y., Bau, H. H. & Zemel, J. N. 1995 Gas flows in micro-channels. *J. Fluid Mech.* **284**, 257–274.

Ho, C.-M & Tai, Y.-C. 1998 Micro-Electro-Mechanical-Systems (MEMS) and fluid flows. *Annu. Rev. Fluid Mech.* **30**, 579–612.

Karim, S. M. & Rosenhead, L. 1952 The second coefficient of viscosity of liquids and gases. *Rev. Mod. Phys.* **24**, 108.

Li, Z.-X., Du, D.-X. & Guo, Z. Y. 2003 Experimental study on flow charactersitics of liquid in circular microtubes. *Microscale Thermophys. Engng* **7**, 253–265.

Macosko, C. W. 1994 *Rheology: Principles, Measurements and Applications.* VCH, NewYork.

Papautsky, I., Ameel, T. & Fraizer, A. B. 2001 A review of laminar single-phase flow in microchannels. *Proc. 2001 ASME Intl Mech. Engng Cong.*, New York.

Poiseuille, J.-L. 1841 Reserches expérimentales sur le mouvement des liquides dans le tubes de très petits diamètres. *Comptes Rendus* **11**, 961.

Prud'homme, R. K., Chapman, T. W. & Bowen, J. R. 1986 Laminar compressible flow in a tube. *Appl. Sci. Res.* **43**, 67–74.

Schwartz, L. W. 1987 A perturbation solution for compressible viscous channel flow. *J. Engng Maths* **21**, 69–86.

Shapiro, A. H. 1953 *The Dynamics and Thermodynamics of Compressible Fluid Flow, Vol. I.* The Roland Press Co., New York.

Stokes, G. 1845 On the theories of the internal friction of fluids in motion, and of the equilibrium and motion of elastic solids. *Trans. Camb. Phil. Soc.* **8**, 287.

Van Dyke, M. 1970 Entry flow in a channel. *J. Fluid Mech.* **44**, 813–823.

Vrentas, J. S., Duda, J. L. & Bargeron, K. G. 1967 Effect of axial diffusion of vorticity on flow development in circular conduits: Part I. Numerical solutions. *AIChE J* **13**, 837–844.

Wilson, S. D. R. 1971 Entry flow in a channel. Part 2. *J. Fluid Mech.* **46**, 787–799.

Zohar, Y., Lee, S. Y. K., Lee, W. Y., Jiang, L. & Tong, P. 2002 Subsonic gas flow in a straight and uniform microchannel. *J. Fluid Mech.* **472**, 125–151.